HHS Public Access

Author manuscript

Pain. Author manuscript; available in PMC 2024 November 01.

Published in final edited form as:

Pain. 2023 November 01; 164(11): 2501–2515. doi:10.1097/j.pain.0000000000002956.

Evolving acidic microenvironments during colitis provide selective analgesic targets for a pH-sensitive opioid

Claudius E. Degro[1,2,*], **Nestor Nivardo Jiménez-Vargas**[1,*], **Quentin Tsang**[1], **Yang Yu**[1], **Mabel Guzman-Rodriguez**[1], **Elahe Alizadeh**[3], **David Hurlbut**[1,4], **David E. Reed**[1], **Alan E. Lomax**[1], **Christoph Stein**[5], **Nigel W. Bunnett**[6,7,#], **Stephen J. Vanner**[1,#]

[1]Gastrointestinal Diseases Research Unit, Kingston General Hospital, Queeńs University, Kingston, Ontario, Canada

[2]Department of General and Visceral Surgery, Charité – Universitätsmedizin Berlin, corporate member of Freie Universität Berlin and Humboldt-Universität zu Berlin, Campus Benjamin Franklin, Hindenburgdamm 30, 12203 Berlin, Germany

[3]Queen's Cardiopulmonary Unit (QCPU), Translational Institute of Medicine (TIME), Department of Medicine, Queen's University, Kingston, Ontario, Canada

[4]Department of Pathology and Molecular Medicine, Queeńs University, Kingston, Ontario, Canada

[5]Department of Experimental Anaesthesiology, Charité – Universitätsmedizin Berlin, corporate member of Freie Universität Berlin and Humboldt-Universität zu Berlin, Campus Benjamin Franklin, Hindenburgdamm 30, 12203 Berlin, Germany

[6]Department of Molecular Pathobiology, New York University College of Dentistry, New York, New York, USA

[7]Department of Neuroscience and Physiology, Neuroscience Institute, Grossman School of Medicine, New York University, New York, New York, USA

Abstract

Targeting the acidified inflammatory microenvironment with pH-sensitive opioids is a novel approach for managing visceral pain while mitigating side effects. The analgesic efficacy of pH-dependent opioids has not been studied during the evolution of inflammation, where fluctuating tissue pH and repeated therapeutic dosing could influence analgesia and side effects. Whether pH-dependent opioids can inhibit human nociceptors during extracellular acidification is unexplored. We studied the analgesic efficacy and side effect profile of a pH-sensitive fentanyl analog, (±)-N-(3-fluoro-1-phenethylpiperidine-4-yl)-N-phenyl propionamide (NFEPP) during the evolution of colitis induced in mice with dextran sulphate sodium. Colitis was characterized by granulocyte infiltration, histological damage and acidification of the mucosa and submucosa at sites of immune

Corresponding author: Dr. Stephen J. Vanner, GI Diseases Research Unit, Kingston General Hospital, 78 Stuart St., K7L 2V7 Kingston, Ontario, Phone: 613.549.6666 ×6518, stephen.vanner@kingstonhsc.ca.

*These authors contributed equally to this manuscript

#These authors contributed equally to this manuscript

Conflict of Interest Statement: The authors have no conflict of interest to declare. The Charité Universitätsmedizin Berlin has filed US patent 14/239,461 on pH-dependent opioid ligands

Patient consent for publication: Not required

cell infiltration. Changes in nociception were determined by measuring visceromotor responses to noxious colorectal distension in conscious mice. Repeated doses of NFEPP inhibited nociception throughout the course of disease with maximal efficacy at the peak of inflammation. Fentanyl was antinociceptive regardless of the stage of inflammation. Fentanyl inhibited gastrointestinal transit, blocked defaecation and induced hypoxemia whereas NFEPP had no such side effects. In proof-of-principle experiments, NFEPP inhibited mechanically-provoked activation of human colonic nociceptors under acidic conditions mimicking the inflamed state. Thus, NFEPP provides analgesia throughout the evolution of colitis with maximal activity at peak inflammation. The actions of NFEPP are restricted to acidified layers of the colon, without common side effects in normal tissues. NFEPP could provide safe and effective analgesia during acute colitis, such as flares of ulcerative colitis.

INTRODUCTION

Abdominal pain is a major cause of morbidity for patients suffering from inflammatory bowel disease (IBD), with nearly 50% of patients reporting pain [38]. Adequate acute pain control in IBD patients relies largely on the administration of opioids, with up to 62% of patients receiving opioids while hospitalized and 21% as outpatients [29].

The actions of opioids are mediated by a subfamily of transmembrane G-protein-coupled receptors: μ-, ∂- and κ-opioid receptors (MORs, DORs, KORs). Activation of these receptors reduces the excitability of nociceptive, spinal and supraspinal neurons and leads to effective analgesia [9,43]. While opioids are the most potent analgesics for acute pain, the ubiquitous expression of opioid receptors at both central and peripheral sites invariably leads to serious on-target side effects (i.e., activation of opioid receptors in all tissues in the body). In the gastrointestinal tract, inhibition of motility and secretion causes constipation, nausea and bloating, resulting in significant morbidity [13,44]. In the central nervous system, sedation and respiratory depression can be life-threatening in hospitalized patients and chronic opioid users [2,23].

An approach to mitigating the on-target side effects has been to modify the pKa of opioids such that they preferentially activate opioid receptors in acidic tissues, such as at sites of inflammation and cancer [42]. We recently studied the pH-sensitive opioid analogue (±)-N-(3-fluoro-1-phenethylpiperidine-4-yl)-N-phenyl propionamide (NFEPP) as a strategy to inhibit nociception in the inflamed intestine without affecting healthy tissues with normal extracellular pH. This fluorinated fentanyl analogue has a lower pKa than the parent compound, facilitating a preferential activation of MORs in the acidic environment of inflamed tissues [40]. We found that a single dose of NFEPP inhibited visceral hyperalgesia in the inflamed colon with similar efficacy to fentanyl, without the side effects of respiratory depression, sedation or constipation [20]. Similar findings have been reported for other models of inflammatory pain [34,40]. However, the analgesic properties of NFEPP have not been studied during the evolution of inflammation, where alterations in tissue pH during the initiation and resolution of disease and repeated dosing could affect analgesic efficacy and occurrence of on-target side effects. The effects of colitis on acidification at the cellular level are unexplored. Whether NFEPP has pH-dependent inhibitory actions on human colonic

nociceptors has not been examined. Herein, we investigated the antinociceptive actions and on-target side effects of repeated dosing of NFEPP during the course of inflammation in a preclinical mouse model that mimics acute episodes of ulcerative colitis. We related the antinociceptive efficacy of NFEPP to acidification at the cellular level. Observations of the effects of extracellular acidification on antinociceptive actions in human colonic nociceptors advance NFEPP as a therapy for IBD pain.

METHODS

Animals

Male C57BL/6 mice (6–8 weeks) were obtained from Charles River Laboratory and kept in a light (12 h cycle) and temperature (22°C) controlled environment with free access to food and water. Mice were randomly assigned to treatment groups and investigators were blinded to experimental regimens. Experiments on animals and animal handling were in accordance with the Canadian Council of Animal Care and approved by the Queen's University Animal Care Committee.

Chemicals and pharmacological drugs

NFEPP is a fluorinated analogue of fentanyl, as previously described [20,40]. Fentanyl citrate was obtained from Sandoz and naloxone hydrochloride from Teligent. Acetylcholine (ACh) chloride (TLC) and naloxone hydrochloride dihydrate (TLC) were purchased from Sigma Aldrich (St Louis, MO).

Dextran sulphate sodium (DSS)- induced colitis

Acute colitis in mice was induced by administration of 2.5% (w/v) DSS (MW: 165.192 g/mol, Cat J14489–22, Thermo Fisher Scientific) diluted in drinking water for 5 days (2.5% DSS protocol) followed by normal water [20,32,51].

Telemetric transmitter implantation and visceromotor responses (VMRs) to colorectal distension (CRD)

Surgical procedures and measurements of VMRs to CRD were performed as previously described [20]. Briefly, for telemetric transmitter implantation, mice were anesthetized with isoflurane in 1 l/min oxygen (2–2.5% isoflurane) and treated with tramadol (20 mg/kg s.c.) and bupivacaine (2 mg/kg, i.d.) to counteract pain. A PhysioTel ETA-F10 telemetric transmitter (Data Science International) was implanted into the abdominal cavity with electrode tips sutured onto the external oblique muscle (~5–10 mm apart) to measure electromyographic (EMG) activity. Following surgery, mice received tramadol (20 mg/kg s.c.) and 1 ml NaCl 0.9% s.c. for three post-operative days to support recovery and rehydration. After 8–10 days, mice underwent the 2.5% DSS protocol. Prior to perform VMR recordings, mice were acclimatized in a restrainer for 30 min daily for two days. At the day of recording, mice were anesthetized with isoflurane, placed in a restrainer, and a 4F arterial embolectomy catheter (Fogarty 120804FF, Edwards Lifesciences) was inserted 0.5 cm into the colorectum. After the mice regained consciousness (10–15 min later), the catheter was distended in a stepwise manner (20, 40, 60, 80 μl, duplicate 10 s distensions, 3-min interval between distensions). VMRs were measured 30 min after vehicle

(0.5% dimethyl sulfoxide, DMSO), NFEPP or fentanyl s.c. administrations, unless stated otherwise. VMRs were analysed with Ponemah v6.5 software (Data Science International). Mean basal EMG activity recorded 10 s before CRD was subtracted from the mean EMG activity recorded during the 10 s CRD. Results are expressed as % VMR in proportion to the maximal VMR recorded after vehicle administration (baseline) in the same mouse (baseline recording 4 hours prior to vehicle duplicate, NFEPP or fentanyl administration).

Study design of opioid treatments

After application of 2.5% DSS for 5 days, mice were switched to normal water (day 1) and experiments were then performed as follows:

Cohort 1: Mice were randomly assigned to NFEPP, fentanyl (each opioid at 0.4 mg/kg s.c.) or vehicle (0.5% DMSO s.c.) treatment groups. Experiments commenced at day 3, based on previous DSS colitis studies showing a robust colonic inflammation after 2 days of normal water [20,25,26], and consisted of s.c. injections administered for 5 days BID (*bis in die*, twice daily: 11am and 5pm) until day 7 followed by a final injection in the morning of day 8. Previous studies have shown that fentanyl analgesia persists >4 hours after s.c. injection [21].

CT- group: Oral contrast- enhanced CT scans were performed at day 3 (pre-treatment, baseline) and at day 8 (1 hour after the last drug injection). At day 3 and day 6, defaecation was assessed over 1 hour immediately after each drug administration. Pulse oximeter experiments were performed at day 4 and day 7 after each drug administration.

VMR- group: VMR recordings were performed at day 3 (after the first drug injection) and at day 8 (after the last drug injection) in response to stepwise CRDs (20, 40, 60, 80 µl). A baseline VMR recording (0.5% DMSO s.c.) was first performed in each group at day 3 and was used as a reference to characterize the VMRs at day 3 and at day 8 after drug administration, individually within each treatment group. VMRs during acute DSS colitis did not change significantly over time (Fig. 1).

Mice of the CT- and VMR- group were used for isometric tension recordings of colonic longitudinal muscle contractile activity or additional pulse oximeter experiments (each opioid at 0.8 mg/kg s.c.) at day 8 after the above-described experiments.

Cohort 2: NFEPP (0.4 mg/kg) was administered s.c. BID (11am and 5pm) starting at day 0 until day 4 followed by a last injection at day 5. VMR recordings in response to 80 µl CRD were performed daily after NFEPP administration starting at day 1 until day 5.

Cohort 3: Locomotor activity, tail immersion assay and pulse oximeter experiments were performed in healthy control mice after vehicle (0.5% DMSO s.c.) and NFEPP (0.8 mg/kg s.c.) administration. The same group of mice was then exposed to the 2.5% DSS protocol to induce acute colonic inflammation. Experiments were then repeated at day 4 and day 5 after NFEPP administration (0.8 mg/kg s.c.).

Disease activity index (DAI) assessment

Mice were monitored daily for colitis disease activity starting at day 1 after the 2.5% DSS protocol until the end of each experiment. The DAI, used in this study, has been previously described [18] and included stool consistency, presence of faecal blood and change in body weight (compared to the body weight one day before starting the 2.5% DSS protocol) to assess the following score: *Stool consistency: 0 = normal, 1 = moist and sticky, 2 = soft, 3 = diarrhoea; stool blood: 0 = normal, 1 = brown reddish colour, 2 = visible blood, 3 = rectal bleeding; body weight loss: 0 = 0–1%, 1 = 1–5%, 2 = 5–10%, 3 = >10%.* Each category was then added up to calculate the final DAI.

Colonic inflammation

Colonic inflammation was assessed by quantification of myeloperoxidase (MPO) activity [24] and by evaluation of haematoxylin and eosin (H&E) stained tissue sections of healthy control and DSS colitis mice. Histological damage of the entire colon wall was assessed, as previously described [20], using a modified scoring: 0 = normal, 1 = damage limited to mucosa, 2 = ulceration limited to submucosa, 3 = focal transmural inflammation and ulceration, 4 = extensive transmural ulceration and inflammation, and 5 = extensive transmural ulceration and inflammation involving the whole section [47].

Whole colon tissue pH measurement

Colonic pH was measured as previously described [20]. Healthy control and DSS colitis mice were euthanized and the colon was excised. After flushing with Krebs solution to remove the intraluminal content, the colon was cut into 2–3 mm flat segments. Tissues were consequently incubated in 20 μM SNARF 5F-5 (and 6) carboxylic acid (Molecular Probes) in phosphate- buffered saline (PBS, in mM: 10 $NaHPO_4$, 2.7 KCl, 137 NaCl, 25 Glucose, pH 7.2) for one hour at 37°C and then washed in PBS (pH 7.4). Tissue SNARF fluorescence was measured (488 nm excitation, 580 and 640 nm emission; Spectra MaxM3) and acquired data were processed using SoftMax Pro 6.5 software (Molecular Devices). Tissue fluorescence (ratio 580/640 nm) conversion to pH was achieved by comparison with a standard curve of SNARF fluorescence in NIH-3T3 cells (1.2×10^6 cells per 0.1 ml, in PBS; pH 5.2 – 8.0 with 0.4 increments).

pH low insertion peptide (pHLIP) imaging

At day 4 after the 2.5% DSS protocol, healthy control and DSS colitis mice received a tail vein injection of a Cyanin (Cy)-7 labelled pHLIP (40 μM, 100 μl: [N>C: AC-(Cy7)-DDQNPWRAYLDLLFPTDTLLLDLLW-DLys-DLys], CPC Scientific Inc). Then, 6–10 hours after injection, mice were euthanized and the colon, small intestine, heart, brain, liver and lung were immediately excised and fixed in 10% formaldehyde overnight. Tissues were then treated with 30% sucrose in PBS (pH 7.4) for cryopreservation (24 hours), before embedding in an optimal cutting temperature (OCT) compound (Tissue-Tek, CA, USA) combined with liquid nitrogen freezing to prepare 9 μm thick slices using a Cryostat (CryoStar NX50, Thermo Fisher Scientific). Tissue slices were then blocked for one hour in a solution containing 2% bovine serum albumin (BSA), 5% normal goat serum and 0.5% Triton X-100 in PBS followed by incubation with a sheep anti-

Cy-Fluorescein isothiocyanate (FITC)-conjugated antibody (1:100, Abcam/ab7628, diluted in PBS containing 1% BSA) overnight. Finally, tissue slices were rinsed in PBS and mounted in a liquid mounting medium formulated with 4′,6-diamidino-2-phenylindole (DAPI, ProLong Gold antifade reagent with DAPI, Thermo Fisher Scientific) before cover-slipped. The presence of DAPI (emission: 455 nm) and FITC (emission: 518 nm) immunofluorescence was then tested by confocal microscopy (Leica TCS SP8, Leica Microsystems, Concord, ON, CA). pHLIP-FITC particle analysis of colon sections was performed based on x10 magnification images (HC PL APO CS2 10x, NA 0.40) by normalizing the number of pHLIP-FITC particles within the mucosa/submucosa and muscle layer against the DAPI density (no. of DAPI positive cells/mm^2) within the same area. The average value of 2–3 different colon sections per mouse was used for further analysis.

In-vivo Micro-Computed Tomography (micro-CT)

Micro-CT images were acquired exploiting VECTor^{4}CT pre-clinical imaging system (MILabs B.V., Utrecht, Netherlands) equipped with a cone beam X-ray CT scanner. The X-ray source rotated around a fixed bed allowing the mouse to be kept in a horizontal position during the scan. Mice were anesthetized with isoflurane in 1 l/min oxygen (2–2.5% isoflurane during the scan) and image acquisition was immediately started after tail vein injection of 200 µl iohexol (300 mg/ml Omnipaque™; GE Healthcare, Princeton, NJ, USA) to increase the abdominal contrast. Measurements were carried out with an acceleration voltage of 50 kVp and an X-ray tube current of 430 µA in an accurate total-body mode to take 720 projections over a 360° scan with 40 ms exposure time. CT images were consequently processed using MILabs reconstruction software implementing a Hann filter of 50 mm voxel grid to generate 3-dimensional (3D) CT images with a slice thickness of 30 µm. A post hoc Gaussian filter of 100 µm was additionally applied to a subset of images using PMOD 3.9 software (PMOD Technologies Ltd., Zurich, Switzerland). Image quantification including gastrointestinal transit (GIT) analysis and diameter calculation was then performed based on axial, coronal and sagittal projections using the Fiji software package (https://imagej.net) and 3D image rendering was finally fulfilled with the OsiriX Lite DICOM Viewer [36].

CT-based GIT scoring and colonic diameter calculation

To assess the CT-based GIT, mice were orally gavaged with 0.2 ml barium sulphate (0.7 g/ml, E-Z-HD, E-Z-EM Canada Inc, Qc, CA) three hours prior to each CT scan. After image acquisition and processing, a scoring system was then applied to describe the location of the leading front of the barium sulphate bolus within the gastrointestinal tract: 0 = stomach and duodenum, 1 = mid small intestine, 2 = terminal ileum, 3 = cecum, 4 = colon, 5 = rectum and expelled. The extent of the large intestine was assessed by calculating the maximal diameter of the cecum and colon based on axial, coronal and sagittal projections using the Fiji software package (https://imagej.net). The largest diameter measured was used for further analysis.

Defaecation

Following s.c. administration of NFEPP, fentanyl (each opioid at 0.4 mg/kg) or vehicle (0.5% DMSO), faecal pellets were counted over one hour. The total number of pellets was used to compare between groups and time points.

Isometric tension recordings and electrical field stimulation (EFS)

Mice were anesthetized with isoflurane and euthanized by cervical dislocation. 1 cm long segments of the mid-colon were subsequently excised, dissected from the mesentery and flushed from the luminal content. Tissue samples were then transferred into organ bath recording chambers (Radnoti, CA, USA) containing carbogenated (95% O_2/ 5% CO_2) Krebs solution (in mM: 118 NaCl, 4.7 KCl, 2.5 $CaCl_2$, 1.2 $MgCl_2$, 25 $NaHCO_3$, 1.2 NaH_2PO_4, 11 Glucose, pH 7.4), warmed to 37°C and changed every 20 min. Colon segments were placed in a vertical position, aligned with the longitudinal muscle and stretched between a glass hook and an isometric force transducer (MLT 0201/RAD, AD Instruments Inc., CO, USA) using silk suture 5–0. Specimens were allowed to equilibrate for 45 min under a pre-tension of 1 g before starting experiments. Experimental protocols included spontaneous activity recordings over a 30 min period to assess frequency and amplitude (baseline-to-peak difference) of spontaneous contractions and to calculate the basal tone defined as the average resting tension between spontaneous contractions. Subsequently, neurogenic induced contractions were provoked via EFS through two horizontal platinum ring electrodes (Radnoti, CA, USA) using a multi-channel stimulator with automation control system (RADSTIM, Radnoti, CA, USA). Pulse trains of 1, 3, 5 and 10 Hertz (Hz) were applied in 3 min intervals to elicit neurogenic induced contractions (EFS parameters: 32 V, 0.5 ms pulse width, 10 s duration) measured as the difference between baseline and peak amplitude. The average of the contractions elicited by two subsequent EFS trains was used for further analysis. In a subset of experiments, naloxone hydrochloride (10 μM) was additionally applied to the organ bath and EFS was repeated after a 5 min wash-in period. Stimulation parameters were set based on preceding experiments showing an abolishment of contractile responses to EFS in the presence of 1 μM tetrodotoxin, indicating no or little effect on direct smooth muscle depolarization (data not shown). Finally, contractility of the smooth muscle was assessed through bath application of ACh chloride in cumulative logarithmic increasing concentrations (10^{-10} – 10^{-3} M, 2 min intervals). All signals were filtered online at 50 Hz and recorded at 1 kHz using LabChart 8.1.10 software (AD Instruments Inc., CO, USA). Tension was normalized against the weight of the tissue used, expressed as g/mg tissue. Data was analysed offline using Clampfit 10.7 software.

Pulse oximeter measurements

Heart rate and blood oxygen saturation were measured in anesthetized mice (1.5% isoflurane) on a heating pad (37°C) using a paw pulse oximeter (Mouse STAT Jr., Kent Scientific). After a 15 min baseline recording, mice were administered NFEPP, fentanyl or vehicle (0.5% DMSO) s.c. Data were subsequently collected every 15 min over one hour.

Tail immersion assay

Mice were acclimatized to the experimental room for one hour and placed in a restrainer. The distal 3 cm of the tail was immersed in a water bath maintained at 52°C. The latency to tail withdrawal (rapid flick) was subsequently video recorded. The cut-off time was set to 10 s to prevent any damage to the tail. Withdrawal latency was measured before and 10 min after NFEPP (0.8 mg/kg) or vehicle (0.5% DMSO) s.c. administration.

Locomotor activity

Mice were acclimatized to the experimental room for one hour prior to each experiment. Locomotor activity was then tested by placing the mice in an open field apparatus (45×45 cm, Harvard Apparatus). Locomotion was assessed by video footages and data were processed using the Smart Video Tracking System V3.0 (Panlab) software. Distance travelled, speed and resting time were recorded over 10 min after NFEPP (0.8 mg/kg) or vehicle (0.5% DMSO) s.c. administration. Repeated locomotor activity experiments in the same mice were performed 7 days apart to prevent habituation to the open field apparatus.

Human extracellular afferent nerve recordings

Colon specimens (descending and sigmoid colon) were obtained from 3 patients (1 male, 2 female) who underwent left hemicolectomy at the Kingston General Hospital, Queeńs University, Kingston, Ontario, CA. All participants signed a written informed consent and experiments were approved by the Queeńs University Human Research Ethics Committees (#6015649). Afferent nerve recordings in human colon preparations were performed as previously described [49]. Colon sections were opened and pinned flat with the mucosal layer face down in a tissue bath perfused with carbogenated (95% O_2/ 5% CO_2) pH 7.4 Krebs solution (in mM: 120 NaCl, 25 $NaHCO_3$, 1.2 $MgSO_4$, 1.2 KH_2PO_4, 11.7 Glucose, 2.0 $CaCl_2$). Mesenteric nerve bundles in the mesentery were identified and aspirated into a glass pipette containing a recording electrode. The receptive fields of the identified nerves were localized by systematically stroking the mesentery and serosa with a brush. Afferents that were responsive to von Frey filament (VFF) probing (10 g), but were not responsive to stretch, were used for further experiments and considered nociceptors. After a 30 min stabilization period, pH 6.5 Krebs solution (adjusted with hydrochloride acid and without carbogen) was applied to the tissue bath for 10 min followed by VFF probing (3 times, 3 s each, 10 g). Next, colon preparations were superfused with NFEPP (300 nM) for 10 min in pH 6.5 Krebs solution and VFF probing was repeated. Thereafter, washout was performed for 20 min with carbogenated pH 7.4 Krebs solution, followed by a final VFF probing. Single units were analysed offline using the Spike 2 software (Version 7, Cambridge Electronic Design).

Statistics

Group differences were analysed using either one or two-way ANOVA with Tukeýs or Bonferronís post hoc test, unless stated otherwise. Non-parametric data was compared with either the Kruskal-Wallis or Friedman test combined with Dunńs post hoc test. A p-value <0.05 was assigned to be statistically significant. Data are shown as mean ± SEM.

RESULTS

Repeated NFEPP administration has antinociceptive activity that is maintained throughout the evolution of colitis

To assess the antinociceptive effects of repeated administration of NFEPP during colitis, equivalent doses of NFEPP or fentanyl (0.4 mg/kg s.c.) or vehicle (0.5% dimethyl sulfoxide, DMSO s.c.) were administered twice daily (*bis in die*, BID) between day 3 and day 8 (Fig. 1 A, cohort 1). VMRs to stepwise CRDs (20, 40, 60, 80 μl) were measured at day 3 and day 8 and did not change during colitis after vehicle injection ($p=0.48$, N=4, two-way ANOVA; Fig. 1 B). However, NFEPP significantly inhibited VMRs over the entire course of colitis (day 3: 74.7 ± 10.8% reduction, $p<0.001$; day 8: 40.5 ± 13.4% reduction, $p<0.001$, N=5, all compared to baseline at 80 μl, two-way ANOVA, Tukeý s test; Fig. 1 C). Nevertheless, the analgesic effect of NFEPP was less at day 8 compared to day 3 (80 μl CRD: $p<0.01$, two-way ANOVA, Tukeý s test). Fentanyl inhibited VMRs at day 3 and day 8 to a similar extent (day 3: 94.6 ± 3.2% reduction, $p<0.001$; day 8: 100% ± 0.0% reduction, $p<0.001$, N=4, all compared to baseline at 80 μl, two-way ANOVA, Tukeý s test; Fig. 1 D). Thus, repeated administrations of NFEPP provide effective antinociceptive actions over the course of acute colitis and this inhibition is blocked by naloxone hydrochloride (Supplementary digital content Fig. 1), as shown in our previous studies [40].

Antinociceptive actions of NFEPP are closely related to the degree of inflammation during colitis

Since NFEPP preferentially activates MORs in the acidified microenvironment of actively inflamed tissues, the decline in efficacy at 8 days might be related to a resolution of inflammation. We therefore investigated whether the antinociceptive effects of NFEPP reflect the degree of inflammation during the evolution of colitis. Daily assessment of DAI revealed that inflammation increased from 1 to 4 days after initial DSS and then declined from days 5 to 8 ($p<0.001$, N=15–43, Kruskal-Wallis test; Fig. 2 A). Consequently, for histological as well as molecular studies of inflammation and tissue pH measurements, colon samples were collected at three different time points reflecting the initiation, peak and resolution of the inflammatory course (days 2, 5, 8, respectively). Histological damage was predominantly localized in the mucosal and submucosal layer and also demonstrated a change in the degree of inflammation over time (Fig. 2 B). Colon damage score was greatest at day 5 ($p<0.001$, N=9) and lower at day 2 ($p<0.05$, N=10) and day 8 ($p<0.01$, N=7, all compared to healthy control, Kruskal-Wallis test, Dunńs test; Fig. 2 C). Colonic MPO activity, an indicator of granulocyte infiltration, was significantly increased at all three times, but also peaked at day 5 (MPO activity: 4.6 ± 0.9 U/mg tissue, $p<0.001$, N=9, compared to healthy control, Kruskal-Wallis test, Dunńs test; Fig. 2 D). Consistent with these findings, colonic pH was lowest at day 5 (pH 6.3 ± 0.05, $p<0.01$, N=5, compared to healthy control, Welchś ANOVA, Dunnett T3 test; Fig. 2 E). To relate these measures of evolving inflammation during colitis to the antinociceptive effects of NFEPP, mice with DSS colitis were treated daily with NFEPP (0.4 mg/kg s.c. BID) during the initiation of disease activity for 6 days and VMRs to CRD (80 μl only) were measured each day (Fig. 2 F, cohort 2). NFEPP did not affect VMRs at day 1, reduced VMRs at day 2, 3 and 4, and maximally inhibited VMRs at day 5 ($p<0.05$, N=5, compared to baseline, Friedman test,

Dunńs test; Fig. 2 F, bar chart). Thus, the maximal antinociceptive action coincides with the peak of inflammation and tissue acidification, in line with the preferential ability of NFEPP to activate MORs in acidified extracellular environments.

Localization of sites of acidification in the inflamed colon using pHLIP reveals tissue-specific pH gradients

pHLIPs allow identification of sites of acidification at the cellular level [39,48]. While soluble at physiological pH, protonation of these specialized peptides at low pH leads to a subsequent insertion into biological membranes thus allowing target specificity for cells located in acidic regions [3]. To reveal acidification at the cellular level of the inflamed colon, we administered a Cy-labelled pHLIP via tail vein injection. At the peak of inflammation in DSS colitis (days 4–5), the pHLIP signal was predominantly identified in the mucosal and submucosal layer, whereas much less signal was detected in the adjacent muscle layer (Fig. 3 A). Analysis of pHLIP density reflected a spatially restricted acidification within the inflamed colon wall (pHLIP-FITC/(DAPI/mm^2): mucosal/submucosal layer: 34.1 ± 6.6 vs. muscle layer: 7.1 ± 2.3, $p<0.01$, N=8, paired t-test; Fig. 3 B). Analysis of the subcellular localization of pHLIP particles revealed a perinuclear signal suggesting insertion into biological membranes in line with their proposed mechanism (Supplementary digital content Fig. 2). In control experiments, fluorescent signals could neither be detected in DSS colitis mice without prior pHLIP injection (Fig. 3 C) nor in the colon of healthy control mice after pHLIP administration (Fig. 3 D). To further validate the specificity of pHLIP for acidic environments, we examined its signal in additional extra-intestinal organs of DSS colitis mice and could not detect pHLIP particles in these areas except for sporadic appearances along blood vessels (e.g., heart, liver; Supplementary digital content Fig. 3). H&E stained sections of the same area revealed a distinctive overlap of the identified pHLIP signal with infiltrating inflammatory cells (Fig. 3 E). Thus, colitis is associated with acidification of mucosal and submucosal tissues at sites of infiltration of inflammatory cells. Nociceptors expressing MORs innervate these regions of the intestine [6,16] facilitating a highly specific and restricted NFEPP mediated inhibition.

Repeated NFEPP application does not inhibit GIT and defaecation during colitis

To examine the effect of repeated dosing of NFEPP and fentanyl on intestinal motility during colitis, oral contrast-enhanced CT scans were recorded to evaluate GIT and defaecation was assessed. Between day 3 and day 8, equivalent doses of NFEPP or fentanyl (0.4 mg/kg s.c.) or vehicle (0.5% DMSO s.c.) were administered BID (Fig. 4 A, cohort 1, CT- group). Oral contrast-enhanced CT scans were recorded at day 3 (before the first drug injection) and at day 8 (after the last drug injection) three hours after barium sulphate gavage (Fig. 4 B). During acute colitis, GIT was not affected by vehicle injections (day 3 vs. day 8: $p>0.99$, N=5, two-way ANOVA, Bonferroni test; Fig. 4 B, C). Likewise, NFEPP did not alter GIT during the course of acute colitis (day 3 vs. day 8: $p=0.60$, N=5, two-way ANOVA, Bonferroni test) whereas fentanyl reduced GIT by 74% (day 3 vs. day 8: $p<0.05$, N=6, two-way ANOVA, Bonferroni test; Fig. 4 B, C). Similarly, no change in defaecation (number of faecal pellets) was observed after NFEPP administration at day 3 and day 6 (N=6) compared to the vehicle (N=5) group (day 3: $p>0.99$; day 6: $p=0.70$, two-way ANOVA, Bonferroni test) in sharp contrast to fentanyl which completely inhibited

defaecation at day 3 and day 6 (day 6: $p<0.05$, N=6, compared to vehicle, two-way ANOVA, Bonferroni test; Fig. 4 D).

Since treatment with MOR agonists in IBD patients is a risk factor for developing toxic megacolon [22], we calculated the maximal diameter of the colon and cecum based on the acquired CT images. In all three treatment groups, no change of the colon and cecum maximal diameter was observed over the treatment period (Fig. 4 E, F). NFEPP or fentanyl did not affect the colonic MPO activity or histological damage score of cohort 1 (CT- and VMR- group; Supplementary digital content Fig. 4).

To further test whether repeated NFEPP administrations induce an impaired colon contractility and myenteric excitability of the inflamed colon, we additionally measured the colonic longitudinal muscle contractile activity by recording isometric tension during phasic activity, in response to EFS and after bath-application of ACh of mid-colon segments from mice with DSS colitis treated with equivalent doses of NFEPP or fentanyl (0.4 mg/kg s.c) or vehicle (0.5% DMSO s.c.) BID over 6 days (Supplementary digital content Fig. 5).

Repeated NFEPP application during colitis has no effect on blood oxygen saturation and less effect on heart rate than fentanyl

On-target side effects compromising the cardiorespiratory system seriously limit the acute and chronic use of conventional MOR agonists [2,46]. To test whether daily repeated applications of NFEPP cause these side effects in our IBD mouse model, we administered equivalent doses of NFEPP or fentanyl (0.4 mg/kg s.c.) or vehicle (0.5% DMSO s.c.) BID for 6 days and monitored blood oxygen saturation and heart rate (Fig. 5 A, cohort 1). NFEPP did neither affect blood oxygen saturation at day 4 and day 7, nor at day 8 after doubling the initial dose to 0.8 mg/kg, whereas fentanyl significantly reduced blood oxygen saturation at each of these time points compared to baseline ([15 min]: day 4: 85.0 ± 1.5% SpO_2, $p<0.01$, N=6; day 7: 87.5 ± 1.4% SpO_2, $p<0.05$, N=6; day 8: 80.0 ± 2.9% SpO_2, $p<0.001$, N=3, two-way ANOVA, Bonferroni test; Fig. 5 B–D). Both fentanyl and NFEPP reduced the heart rate at day 4, day 7 and at day 8 (Fig. 5 E–G). However, compared to fentanyl, the NFEPP effect was smaller and more transient, with a partial or full recovery after 60 min compared to baseline (day 8: Δ BPM +11.9 ± 14.6 from baseline, $p>0.99$, N=5, two-way ANOVA, Bonferroni test; Fig. 5 G). At 0.8 mg/kg s.c., the maximal decline in heart rate from baseline averaged 31.7% for fentanyl and 16.5% for NFEPP. Within all treatment groups, no differences of heart rate or blood oxygen saturation were observed comparing day 4 with day 7 experiments. Thus, after repeated administration, NFEPP has no effect on blood oxygenation and thus respiration and minimal effect on heart rate compared to fentanyl which markedly reduces both parameters.

High doses of NFEPP do not affect blood oxygen saturation, somatic thermal nociception and locomotion in mice with and without colitis

On-target effects in the central nervous system (e.g., sedation) are frequent limitations of conventional MOR agonists [7,14]. To test whether high doses of NFEPP have central on-target side effects, we administered NFEPP in a concentration of 0.8 mg/kg s.c., a dose approximately 25-fold higher than the ED_{50} of fentanyl for thermal nociception [28].

Experiments were first performed in healthy mice followed by application of the 2.5% DSS protocol in the same set of mice and repetition of central side effects experiments (Fig. 6 A, cohort 3). In healthy mice, NFEPP did not affect somatic thermal nociception, assessed by a tail immersion assay ($p=0.11$, N=8, two-way ANOVA), and had no effect on locomotor behavior, measured by total distance travelled ($p=0.19$, N=7, one-way ANOVA), mean speed ($p=0.19$, N=7, one-way ANOVA) and resting time ($p=0.06$, N=7, one-way ANOVA) in a locomotion open field test (Fig. 6 B–F). After induction of DSS colitis, tail immersion assay and open field experiments were repeated at peak inflammation (days 4–5). As found in healthy mice, NFEPP (0.8 mg/kg) had no effect on thermal nociception nor on locomotor behavior in DSS colitis mice (Fig. 6 B–F). This higher concentration of NFEPP also had no effect on blood oxygen saturation in healthy and DSS colitis mice (N=6; Fig. 6 G). However, as found with repeated dosing of NFEPP at a lower dose (Fig. 5), a single dose of a higher concentration of NFEPP (0.8 mg/kg s.c.) caused a small reduction in heart rate that recovered after 60 min in both, mice with and without colitis (DSS NFEPP [60 min]: Δ BPM +8.9 ± 21.3 from baseline, $p>0.99$, N=6, compared to baseline, two-way ANOVA, Bonferroni test; Fig. 6 H).

NFEPP inhibits colonic nociception in isolated human colon preparations in acidic conditions

To test whether NFEPP also inhibits nociception in human tissues, afferent nerve recordings from mesenteric nerves were made in isolated preparations of the left colon (descending and sigmoid colon) from female and male patients. Colonic nociceptors were identified based on their responsiveness to VFF probing (10 g, serosal or mesenteric probing). Control responses to VFF probing were measured after tissue equilibration (10 min) at pH 6.5. At pH 6.5, NFEPP application (300 nM) to the tissue bath (10 min wash-in) caused a 49% reduction in afferent nerve activity in response to VFF probing compared to pH 6.5 control responses ($p<0.05$, N=3, Friedman test, Dunńs test; Fig. 7 A–C). A subsequent 20 min washout period at pH 7.4 did not provide complete washout of the observed effect. These results show that NFEPP is able to inhibit the activity of human colonic nociceptors in the setting of extracellular acidification that replicates inflammation. These findings, that mirror our previous findings in the mouse colon [20], support the concept of using NFEPP to treat pain associated with IBD, with fewer side effects than conventional opioids such as fentanyl.

DISCUSSION

Opioids are the most effective analgesics for the management of acute pain and are often required for pain management of IBD patients, especially those requiring hospital admission [29]. Patients typically require repeated dosing of analgesics to manage their visceral pain, and they often experience unpleasant on-target side effects and occasionally life-threatening events [2,7,44]. In the current study, we have shown that repeated application of the pH-sensitive opioid NFEPP inhibits visceral nociceptive responses during the evolution of acute colitis in a preclinical model of ulcerative colitis. This antinociceptive action of NFEPP was targeted to sites of inflammation and acidification within the colon and was sustained during the period of inflammation. The common on-target side effects of opioids, such as constipation, delayed GIT, respiratory depression and adverse central effects, were

not observed, even with increased dosing. We strengthened the translational relevance of these findings by demonstrating that NFEPP inhibits human colonic nociceptors in acidified conditions, mimicking the acidic intramural and intraluminal microenvironments found in many human inflammatory disorders such as ulcerative colitis, Crohn's disease, ischemic colitis or colorectal cancer [27,30,37].

NFEPP was designed by modifying fentanyl (hydrogen replacement with fluorine on its piperidine moiety) to decrease its pKa and thereby enable MOR activation preferentially in acidified tissues [20,34,40]. We have extensively investigated the activity of fentanyl and NFEPP at different types of opioid receptors in injured/inflamed versus non-injured/non-inflamed tissues by using μ-, *∂*- and κ- selective antagonists in rats [40] and in mice [4]. NFEPP was selective for MORs. Fentanyl was active in both normal and inflamed tissues, while NFEPP was not active in non-inflamed tissues [4,40]. Based on the chemical structures and on our previous in vivo data, there is no evidence for significant differences in drug distribution between fentanyl, NFEPP and related compounds [4,10,40,41]. Both ligands are lipophilic and will rapidly penetrate the blood-brain- (and other) barriers. We have also thoroughly investigated related compounds with varying pKa values (6.82 – 8.44) in vitro and in vivo in two further papers [10,41]. Finally, our previous studies have shown that the analgesic actions of NFEPP are blocked by the peripherally restricted opioid receptor antagonist naloxone methiodide, demonstrating that these analgesic effects are mediated by activation of peripheral MORs [34,40]. Together, these data indicated that ligands with pKa values close to the pH of inflamed/injured tissues selectively activate peripheral opioid receptors, and that progressively decreasing pKa values correlate with diminishing central adverse effects.

Tissue pH will vary with the degree of inflammation and thus the magnitude of analgesia for a given dose of a pH-sensitive compound would be anticipated to reflect the severity of inflammation. Indeed, we found that NFEPPś antinociceptive effects were greatest at the peak of colonic inflammation, based on DAI, MPO activity, histological scoring and measurements of colonic pH. Together, these findings provide further support for the selective mechanism of action of NFEPP and its clinical utility. Peripheral nociceptive signaling and resulting pain would be greatest at peak inflammation in the clinical course and these results indicate that NFEPP's analgesic activity for a given dose would be maximal at this time point. Although the analgesic actions of NFEPP and fentanyl appear similar at peak inflammation, it is possible that the overall magnitude of analgesia compared to fentanyl, which would also inhibit pain central pathways including the dorsal horn, may be less.

The distribution of inflammation in the tissue layers of the colon resulting from acute DSS colitis also offers insights into the mechanism of action of NFEPP. The inflammation in this self-limiting colitis model is predominantly found in the mucosa and submucosa, as shown by our histological analysis and previous studies [8]. It is generally considered a model of ulcerative colitis [31], as opposed to the transmural inflammation that characterizes Crohn's disease [33]. We localized sites of colonic acidification by using specialized peptides that insert into cell membranes at a low pH, a strategy that was recently validated in cancer models [1] where acidic pH is amongst the lowest observed in tissues [35].

Using Cy-labelled pHLIP, we found its highest accumulation in the colonic mucosal and submucosal layers whereas much less pHLIP was detected in the adjacent muscle layer. These findings are consistent with our histological scores suggesting the greatest inflammation occurred within these regions. The nerve terminals of visceral nociceptors travel into the colon along the arterioles that terminate within the submucosa. Acidosis within the submucosal microenvironment that activates NFEPP with ensuing inhibition of these nerves is highly consistent with the proposed mechanism of action. The lack of acidification of the musculature explains the inability of NFEPP to inhibit GIT and defaecation.

Our study examined male mice due to previous reports demonstrating that female mice show a reduced inflammatory response to DSS consumption compared to male mice [5,15]. Furthermore, our previous studies have shown that opioid responses in visceral DRG neurons did not differ between female and male mice [19,50]. Such findings are consistent with the current evidence on sex-differences in opioid analgesia suggesting sex-specific therapeutic interventions are not warranted [11,12].

The cumulative actions of opioids and their metabolites with repeated dosing could amplify potential on-target side effects or could cause tolerance. Fentanyl caused an inhibition of transit and defaecation, whereas NFEPP had neither an effect on defaecation nor on GIT, even after repeated dosing. These results are consistent with the finding that inflammation and acidification were largely confined to the mucosa and submucosa. Thus, NFEPP activated MORs at these sites as opposed to the muscle layer. Future studies of models of transmural inflammation, which more closely approximates the distribution of inflammation in Crohn's disease, are required to further elucidate NFEPP activity within the gut wall.

We did not detect common on-target side effects in organs outside the gastrointestinal tract after repeated dosing of NFEPP, in contrast to fentanyl. Chronic treatment with NFEPP did not affect blood oxygen saturation at any point during acute colitis. We also showed that acute application of increased doses of NFEPP (multiples of the fentanyl ED_{50} for thermal nociception) had no effect. In contrast, fentanyl caused significant hypoxemia and a reduction of heart rate even at lower doses. Our previous study with a single lower dose of NFEPP (0.2 mg/kg s.c.) revealed no effect on central regulation of locomotion or peripherally on somatic sensory testing whereas fentanyl at the same dose had profound effects [20]. Herein, we also showed that even with doses four times higher than those initially studied, NFEPP had no effect on locomotion and somatic nociception compared to vehicle. We did observe a distinctive inhibition of heart rate with fentanyl and a smaller, transient effect with NFEPP when used at higher doses. While opioid receptor expression is present in the heart [17,45], the explanation for why NFEPP has a transient effect is unclear, but potentially could reflect a small and local acidic microenvironment. Our studies with pHLIP detected a small signal in the heart, whereas nothing was found in the brain or small intestine, but these signals were found along blood vessels and their significance is unclear.

In summary, repeated dosing of NFEPP provides sustained antinociception during the evolution of an acute colonic inflammation and this cumulative dosing does not lead to typical on-target side effects. Due to its pKa that favors acidic environments, the activity

of NFEPP is maximal at peak inflammation when nociceptive stimulation from tissue mediators is greatest and its actions are highly restricted to sites of acidification within the inflamed colon wall. Thus, this novel opioid shows considerable promise to provide targeted, effective and safe analgesia by actions in peripheral nociceptive nerves throughout the course of an acute inflammatory disorder such as occurs in IBD and other chronic remitting inflammatory diseases.

Supplementary Material

Refer to Web version on PubMed Central for supplementary material.

Acknowledgments:

SV, DR, AL were funded by an operating grant from Crohn's and Colitis Canada. NWB was funded by grants from National Institutes of Health (NS102722, DE026806, DK118971, DE029951) and Department of Defense (W81XWH1810431, W81XWH-22-1-0239, Expansion Award). CS was funded by grants from Deutsche Forschungsgemeinschaft (STE 477/19, EXC 2046 AA1-15, FOR 5177, STE 477/21) and Bundesministerium für Bildung und Forschung (01GQ2109A)

Data availability statement:

The data that support the findings of this study are available from the corresponding author upon reasonable request.

REFERENCES

[1]. Adochite RC, Moshnikova A, Carlin SD, Guerrieri RA, Andreev OA, Lewis JS, Reshetnyak YK. Targeting breast tumors with pH (Low) insertion peptides. Mol Pharm 2014;11:2896–2905. [PubMed: 25004202]

[2]. Algera MH, Olofsen E, Moss L, Dobbins RL, Niesters M, van Velzen M, Groeneveld GJ, Heuberger J, Laffont CM, Dahan A. Tolerance to Opioid-Induced Respiratory Depression in Chronic High-Dose Opioid Users: A Model-Based Comparison With Opioid-Naïve Individuals. Clin Pharmacol Ther 2021;109:637–645. [PubMed: 32865832]

[3]. Andreev OA, Dupuy AD, Segala M, Sandugu S, Serra DA, Chichester CO, Engelman DM, Reshetnyak YK. Mechanism and uses of a membrane peptide that targets tumors and other acidic tissues in vivo. Proc Natl Acad Sci U S A 2007;104:7893–7898. [PubMed: 17483464]

[4]. Baamonde A, Menéndez L, González-Rodríguez S, Lastra A, Seitz V, Stein C, Machelska H. A low pKa ligand inhibits cancer-associated pain in mice by activating peripheral mu-opioid receptors. Sci Rep 2020;10.

[5]. Bábíčková J, Tóthová Ľ, Lengyelová E, Bartoňová A, Hodosy J, Gardlík R, Celec P. Sex Differences in Experimentally Induced Colitis in Mice: a Role for Estrogens. Inflammation 2015;38.

[6]. Bagnol D, Mansour A, Akil H, Watson SJ. Cellular localization and distribution of the cloned mu and kappa opioid receptors in rat gastrointestinal tract. Neuroscience 1997;81.

[7]. Bateman JT, Saunders SE, Levitt ES. Understanding and countering opioid-induced respiratory depression. Br J Pharmacol 2021.

[8]. Chassaing B, Aitken JD, Malleshappa M, Vijay-Kumar M. Dextran sulfate sodium (DSS)-induced colitis in mice. Curr Protoc Immunol 2014.

[9]. Corder G, Castro DC, Bruchas MR, Scherrer G. Endogenous and exogenous opioids in pain. Annu Rev Neurosci 2018;41:453–473. [PubMed: 29852083]

[10]. Del Vecchio G, Labuz D, Temp J, Seitz V, Kloner M, Negrete R, Rodriguez-Gaztelumendi A, Weber M, Machelska H, Stein C. pKa of opioid ligands as a discriminating factor for side effects. Sci Rep 2019;9.

[11]. Fillingim RB, King CD, Ribeiro-Dasilva MC, Rahim-Williams B, Riley JL. Sex, Gender, and Pain: A Review of Recent Clinical and Experimental Findings. J Pain 2009;10:447–485. [PubMed: 19411059]

[12]. Fullerton EF, Doyle HH, Murphy AZ. Impact of sex on pain and opioid analgesia: a review. Curr Opin Behav Sci 2018;23:183–190. [PubMed: 30906823]

[13]. Galligan JJ, Sternini C. Insights into the role of opioid receptors in the GI tract: Experimental evidence and therapeutic relevance. Handb Exp Pharmacol 2017;239:363–378. [PubMed: 28204957]

[14]. Gaudreau JD, Gagnon P, Harel F, Roy MA, Tremblay A. Psychoactive medications and risk of delirium in hospitalized cancer patients. J Clin Oncol 2005;23:6712–6718. [PubMed: 16170179]

[15]. Goodman WA, Havran HL, Quereshy HA, Kuang S, De Salvo C, Pizarro TT. Estrogen Receptor α Loss-of-Function Protects Female Mice From DSS-Induced Experimental Colitis. CMGH 2018;5.

[16]. Guerrero-Alba R, Valdez-Morales EE, Jiménez-Vargas NN, Bron R, Poole D, Reed D, Castro J, Campaniello M, Hughes PA, Brierley SM, Bunnett N, Lomax AE, Vanner S. Co-expression of μ and δ opioid receptors by mouse colonic nociceptors. Br J Pharmacol 2018;175.

[17]. He SF, Jin SY, Yang W, Pan YL, Huang J, Zhang SJ, Zhang L, Zhang Y. Cardiac μ-opioid receptor contributes to opioid-induced cardioprotection in chronic heart failure. Br J Anaesth 2018;121:26–37. [PubMed: 29935580]

[18]. Huynh E, Penney J, Caswell J, Li J. Protective effects of protegrin in dextran sodium sulfate-induced murine colitis. Front Pharmacol 2019;10.

[19]. Jaramillo-Polanco J, Lopez-Lopez C, Yu Y, Neary E, Hegron A, Canals M, Bunnett NW, Reed DE, Lomax AE, Vanner SJ. Opioid-Induced Pronociceptive Signaling in the Gastrointestinal Tract Is Mediated by Delta-Opioid Receptor Signaling. J Neurosci 2022;42.

[20]. Jiménez-Vargas NN, Yu Y, Jensen DD, Bok DD, Wisdom M, Latorre R, Lopez C, Jaramillo-Polanco JO, Degro C, Guzman-Rodriguez M, Tsang Q, Snow Z, Schmidt BL, Reed DE, Lomax AE, Margolis KG, Stein C, Bunnett NW, Vanner SJ. Agonist that activates the μ-opioid receptor in acidified microenvironments inhibits colitis pain without side effects. Gut 2021.

[21]. Kalvass JC, Olson ER, Cassidy MP, Selley DE, Pollack GM. Pharmacokinetics and pharmacodynamics of seven opioids in P-glycoprotein-competent mice: Asssessment of unbound brain EC50,u and correlation of in vitro, preclinical, and clinical data. J Pharmacol Exp Ther 2007;323.

[22]. Katagiri N, Sakai R, Izutsu T, Kawana H, Sugino S, Kido K. Postoperative Pain Management in Patients With Ulcerative Colitis. Anesth Prog 2020;67:158–163. [PubMed: 32992337]

[23]. Khanna AK, Bergese SD, Jungquist CR, Morimatsu H, Uezono S, Lee S, Ti LK, Urman RD, McIntyre R, Tornero C, Dahan A, Saager L, Weingarten TN, Wittmann M, Auckley D, Brazzi L, Le Guen M, Soto R, Schramm F, Ayad S, Kaw R, Di Stefano P, Sessler DI, Uribe A, Moll V, Dempsey SJ, Buhre W, Overdyk FJ, Tanios M, Rivas E, Mejia M, Elliott K, Ali A, Fiorda-Diaz J, Carrasco-Moyano R, Mavarez-Martinez A, Gonzalez-Zacarias A, Roeth C, Kim J, Esparza-Gutierrez A, Weiss C, Chen C, Taniguchi A, Mihara Y, Ariyoshi M, Kondo I, Yamakawa K, Suga Y, Ikeda K, Takano K, Kuwabara Y, Carignan N, Rankin J, Egan K, Waters L, Sim MA, Lean LL, Liew QEL, Siu-Chun Law L, Gosnell J, Shrestha S, Okponyia C, Al-Musawi MH, Gonzalez MJP, Neumann C, Guttenthaler V, Männer O, Delis A, Winkler A, Marchand B, Schmal F, Aleskerov F, Nagori M, Shafi M, McPhee G, Newman C, Lopez E, Har SM, Asbahi M, Nordstrom McCaw K, Theunissen M, Smit-Fun V. Prediction of Opioid-Induced Respiratory Depression on Inpatient Wards Using Continuous Capnography and Oximetry: An International Prospective, Observational Trial. Anesth Analg 2020:1012–1024. [PubMed: 32925318]

[24]. Kim JJ, Shajib MS, Manocha MM, Khan WI. Investigating intestinal inflammation in DSS-induced model of IBD. J Vis Exp 2012:1–6.

[25]. Lama A, Provensi G, Amoriello R, Pirozzi C, Rani B, Mollica MP, Raso GM, Ballerini C, Meli R, Passani MB. The anti-inflammatory and immune-modulatory effects of OEA limit DSS-induced colitis in mice. Biomed Pharmacother 2020;129.

[26]. López-Estévez S, Gris G, de la Puente B, Carceller A, Martínez V. Intestinal inflammation-associated hypersensitivity is attenuated in a DSS model of colitis in Sigma-1 knockout C57BL/6 mice. Biomed Pharmacother 2021;143.

[27]. Meyer KA, Kammerling EM, Amtman L, Koller M, Hoffman SJ. pH Studies of Malignant Tissues in Human Beings. Cancer Res 1948;8.

[28]. Minami K, Hasegawa M, Ito H, Nakamura A, Tomii T, Matsumoto M, Orita S, Matsushima S, Miyoshi T, Masuno K, Torii M, Koike K, Shimada S, Kanemasa T, Kihara T, Narita M, Suzuki T, Kato A. Morphine, oxycodone, and fentanyl exhibit different analgesic profiles in mouse pain models. J Pharmacol Sci 2009;111:60–72. [PubMed: 19729873]

[29]. Niccum B, Moninuola O, Miller K, Khalili H. Opioid Use Among Patients With Inflammatory Bowel Disease: A Systematic Review and Meta-analysis. Clin Gastroenterol Hepatol 2021;19:895–907.e4. [PubMed: 32835841]

[30]. Nugent SG, Kumar D, Rampton DS, Evans DF. Intestinal luminal pH in inflammatory bowel disease: Possible determinants and implications for therapy with aminosalicylates and other drugs. Gut 2001;48.

[31]. Okayasu I, Hatakeyama S, Yamada M, Ohkusa T, Inagaki Y, Nakaya R. A novel method in the induction of reliable experimental acute and chronic ulcerative colitis in mice. Gastroenterology 1990;98:694–702. [PubMed: 1688816]

[32]. Park YH, Kim N, Shim YK, Choi YJ, Nam RH, Choi YJ, Ham MH, Suh JH, Lee SM, Lee CM, Yoon H, Lee HS, Lee DH. Adequate Dextran Sodium Sulfate-induced Colitis Model in Mice and Effective Outcome Measurement Method. J Cancer Prev 2015;20.

[33]. Podolsky DK. Inflammatory bowel disease. N Engl J Med. 2002 Aug 8;347(6):417–29. [PubMed: 12167685]

[34]. Rodriguez-Gaztelumendi A, Spahn V, Labuz D, MacHelska H, Stein C. Analgesic effects of a novel pH-dependent m-opioid receptor agonist in models of neuropathic and abdominal pain. Pain 2018;159:2277–2284. [PubMed: 29994988]

[35]. Rohani N, Hao L, Alexis MS, Joughin BA, Krismer K, Moufarrej MN, Soltis AR, Lauffenburger DA, Yaffe MB, Burge CB, Bhatia SN, Gertler FB. Acidification of tumor at stromal boundaries drives transcriptome alterations associated with aggressive phenotypes. Cancer Res 2019;79:1952–1966. [PubMed: 30755444]

[36]. Rosset A, Spadola L, Ratib O. OsiriX: An open-source software for navigating in multidimensional DICOM images. J Digit Imaging 2004;17:205–216. [PubMed: 15534753]

[37]. Schiedler MG. Sigmoid Intramural pH for Prediction of Ischemic Colitis During Aortic Surgery. Arch Surg 1987;122.

[38]. Schirbel A, Reichert A, Roll S, Baumgart DC, Büning C, Wittig B, Wiedenmann B, Dignass A, Sturm A. Impact of pain on health-related quality of life in patients with inflammatory bowel disease. World J Gastroenterol 2010;16:3168–3177. [PubMed: 20593502]

[39]. Sosunov EA, Anyukhovsky EP, Sosunov AA, Moshnikova A, Wijesinghe D, Engelman DM, Reshetnyak YK, Andreev OA. pH (low) insertion peptide (pHLIP) targets ischemic myocardium. Proc Natl Acad Sci U S A 2013;110:82–86. [PubMed: 23248283]

[40]. Spahn V, Del Vecchio G, Labuz D, Rodriguez-Gaztelumendi A, Massaly N, Temp J, Durmaz V, Sabri P, Reidelbach M, Machelska H, Weber M, Stein C. A nontoxic pain killer designed by modeling of pathological receptor conformations. Science (80-) 2017;355:966–969.

[41]. Spahn V, Del Vecchio G, Rodriguez-Gaztelumendi A, Temp J, Labuz D, Kloner M, Reidelbach M, Machelska H, Weber M, Stein C. Opioid receptor signaling, analgesic and side effects induced by a computationally designed pH-dependent agonist. Sci Rep 2018;8.

[42]. Stein C. New concepts in opioid analgesia. Expert Opin Investig Drugs 2018;27:765–775.

[43]. Sternini C, Patierno S, Selmer IS, Kirchgessner A. The opioid system in the gastrointestinal tract. Neurogastroenterol Motil 2004;16:3–16.

[44]. Swegle JM, Logemann C. Management of common opioid-induced adverse effects. Am Fam Physician 2006;74:1347–1354. [PubMed: 17087429]

[45]. Theisen MM, Schlottmann S, August C, Herzog C, Theilmeier G, Maas M, Blumenstiel JM, Weber TP, Van Aken HK, Kaerlein KT. Detection and distribution of opioid peptide receptors in porcine myocardial tissue. Pharmacol Res 2014;84:45–49. [PubMed: 24788078]

[46]. Urman RD, Khanna AK, Bergese SD, Buhre W, Wittmann M, Le Guen M, Overdyk FJ, Di Piazza F, Saager L. Postoperative opioid administration characteristics associated with opioid-induced respiratory depression: Results from the PRODIGY trial. J Clin Anesth 2021;70.

[47]. Wallace JL, Keenan CM. An orally active inhibitor of leukotriene synthesis accelerates healing in a rat model of colitis. Am J Physiol - Gastrointest Liver Physiol 1990;258.

[48]. Yao L, Danniels J, Moshnikova A, Kuznetsov S, Ahmed A, Engelman DM, Reshetnyak YK, Andreev OA. pHLIP peptide targets nanogold particles to tumors. Proc Natl Acad Sci U S A 2013;110:465–470. [PubMed: 23267062]

[49]. Yu Y, Daly DM, Adam IJ, Kitsanta P, Hill CJ, Wild J, Shorthouse A, Grundy D, Jiang W. Interplay between mast cells, enterochromaffin cells, and sensory signaling in the aging human bowel. Neurogastroenterol Motil 2016;28.

[50]. Yu Y, Tsang QK, Jaramillo-Polanco J, Lomax AE, Vanner SJ, Reed DE. Cannabinoid 1 and mu-opioid receptor agonists synergistically inhibit abdominal pain and lack side effects in mice. J Neurosci. 2022 Jul 1:JN-RM-0641–22.

[51]. Zhai Z, Zhang F, Cao R, Ni X, Xin Z, Deng J, Wu G, Ren W, Yin Y, Deng B. Cecropin A alleviates inflammation through modulating the gut microbiota of C57BL/6 mice with DSS-induced IBD. Front Microbiol 2019;10.

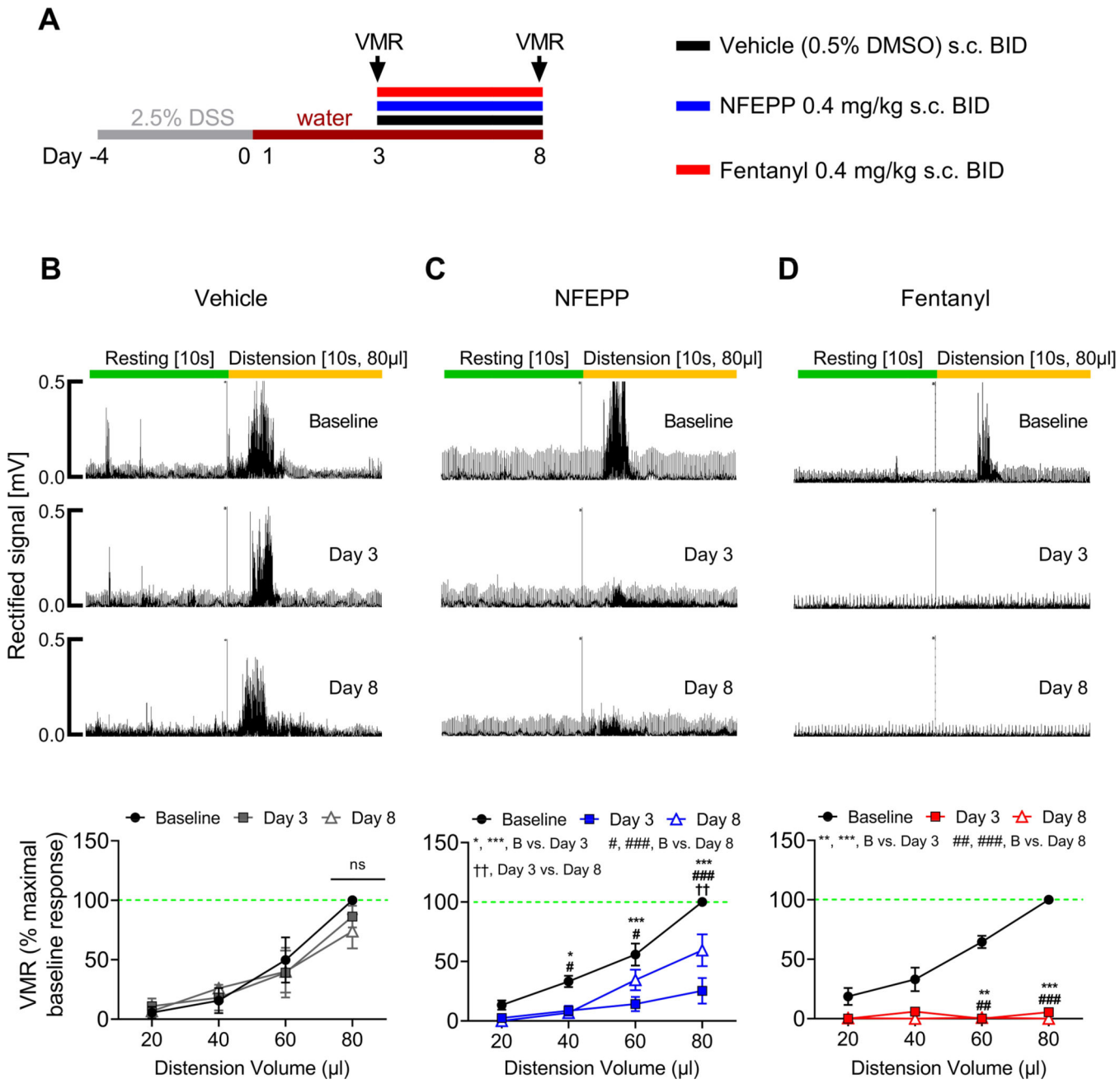

Fig. 1: Effects of repeated NFEPP and fentanyl application on visceromotor responses (VMRs) to colorectal distension during acute DSS colitis.

A. Study design with injection regimen (*color coded*). VMRs were measured at day 3 and day 8. **B-D.** Effects of vehicle (**B**, 0.5% DMSO s.c., p=0.48, N=4), NFEPP (**C**, 0.4 mg/kg s.c., p<0.001, N=5) and fentanyl (**D**, 0.4 mg/kg s.c., p<0.001, N=4) on VMRs to colorectal distension at day 3 and day 8 with representative traces. *Abbreviations: B, baseline. BID, bis in die (twice daily). DMSO, dimethyl sulfoxide. DSS, dextran sulphate sodium. *, # p<0.05. **, ##, †† p<0.01. ***, ### p<0.001. Two-way ANOVA, Tukeýs test.*

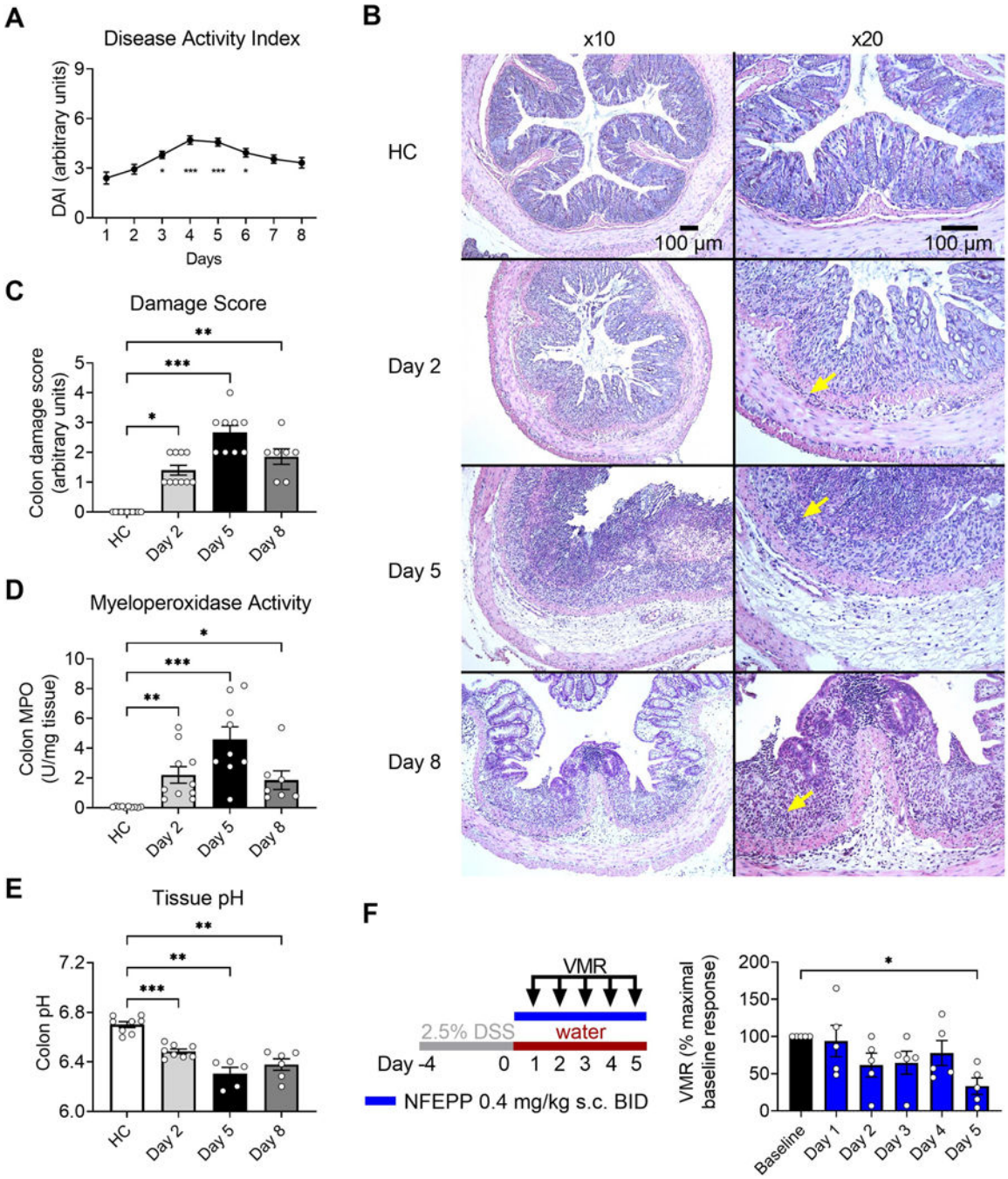

Fig. 2: Changes of colonic inflammation and NFEPP effects on visceromotor responses (VMRs) during acute DSS colitis.

A. DAI of DSS colitis mice over time (N=15–43, combined data of all cohorts, compared to day 1). **B-E**. Histology (**B**, H&E staining), histological damage score (**C**), MPO activity (**D**) and tissue pH (**E**) of the colon from healthy control (HC, N=8–11) and DSS colitis mice (N=5–10) at different time points. Arrows in (**B**) denote infiltrating inflammatory cells. **F.** Study design with injection regimen (*color coded*) and daily VMR measurements (80 µl colorectal distension, day 1 - day 5) after NFEPP administration (0.4 mg/kg s.c.) in DSS

colitis mice (N=5). *Abbreviations: BID, bis in die (twice daily). DAI,* disease activity index. *DSS, dextran sulphate sodium. H&E, haematoxylin and eosin. MPO, myeloperoxidase. * p<0.05. ** p<0.01. *** p<0.001. A, C, D: Kruskal-Wallis test, Dunńs test. E: Welch ANOVA, Dunnett T3 test. F: Friedman test, Dunńs test.*

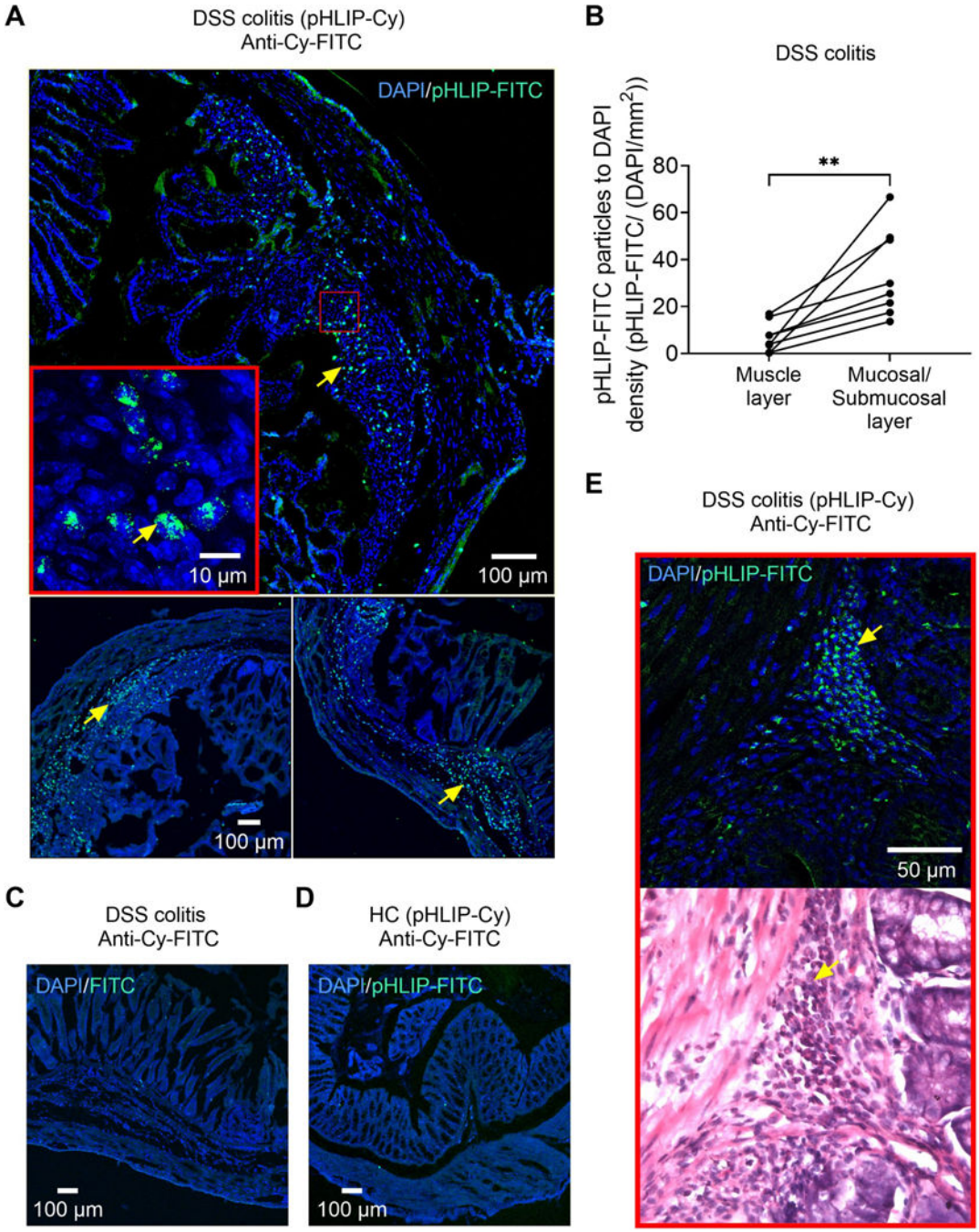

Fig. 3: pHLIP sublocalization in the colon of healthy control and acute DSS colitis mice.

A. DAPI/ anti-Cy-FITC labelling in DSS colitis mice treated with pHLIP (representative images of N= 2 mice). Staining (arrows) is predominantly localized in the mucosal and submucosal layer. Inset shows the subcellular localization of pHLIP. See also Supplementary digital content Fig. 2 for expanded confocal images illustrating the insertion of pHLIP into cell membranes within the inflamed layers of the colon. **B.** pHLIP-FITC particle distribution within the colon wall of DSS colitis mice (N=8). **C.** DAPI/ anti-Cy-FITC labelling in a DSS colitis mouse that was not treated with pHLIP. **D.** DAPI/ anti-Cy-FITC labelling in a

healthy control (HC) mouse treated with pHLIP. **E.** DAPI/ anti-Cy-FITC labelling and H&E staining in a DSS colitis mouse treated with pHLIP. Arrows denote the co-localization of pHLIP particles and infiltrating inflammatory cells. *Abbreviations: Cy, Cyanin. DAPI, 4′,6-diamidino-2-phenylindole. DSS, dextran sulphate sodium. FITC, fluorescein isothiocyanate. H&E, haematoxylin and eosin. pHLIP, pH low insertion peptide. ** p<0.01. Paired t-test.*

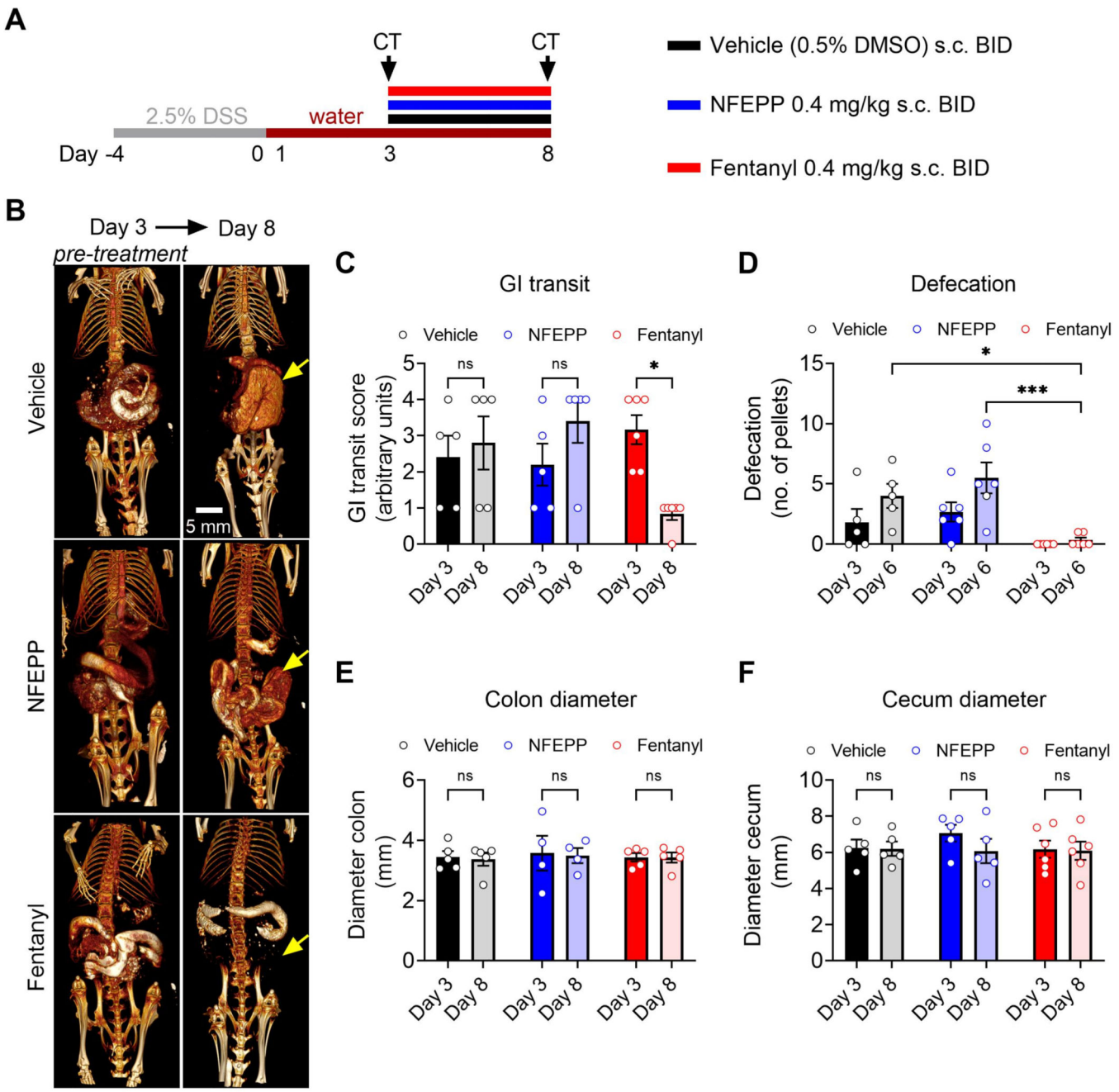

Fig. 4: Effects of repeated NFEPP and fentanyl application on gastrointestinal (GI) transit and defaecation during acute DSS colitis.

A. Study design with injection regimen (*color coded*). **B.** Oral contrast- enhanced CT scans before (day 3, drug naive) and after (day 8) repeated dosing of vehicle (0.5% DMSO s.c., N=5), NFEPP (0.4 mg/kg s.c., N=5) or fentanyl (0.4 mg/kg s.c., N=6) BID. Arrows denote the cecum. **C.** Effects of NFEPP and fentanyl on CT-based GI transit. **D.** Effects of NFEPP and fentanyl administration (each opioid at 0.4 mg/kg s.c.) on defaecation. **E-F.** Effects of NFEPP and fentanyl on colon diameter (**E**) and cecum diameter (**F**). *Abbreviations: BID, bis*

*in die (twice daily). DMSO, dimethyl sulfoxide. DSS, dextran sulphate sodium. * p<0.05. *** p<0.001. Two-way ANOVA, Bonferroni test.*

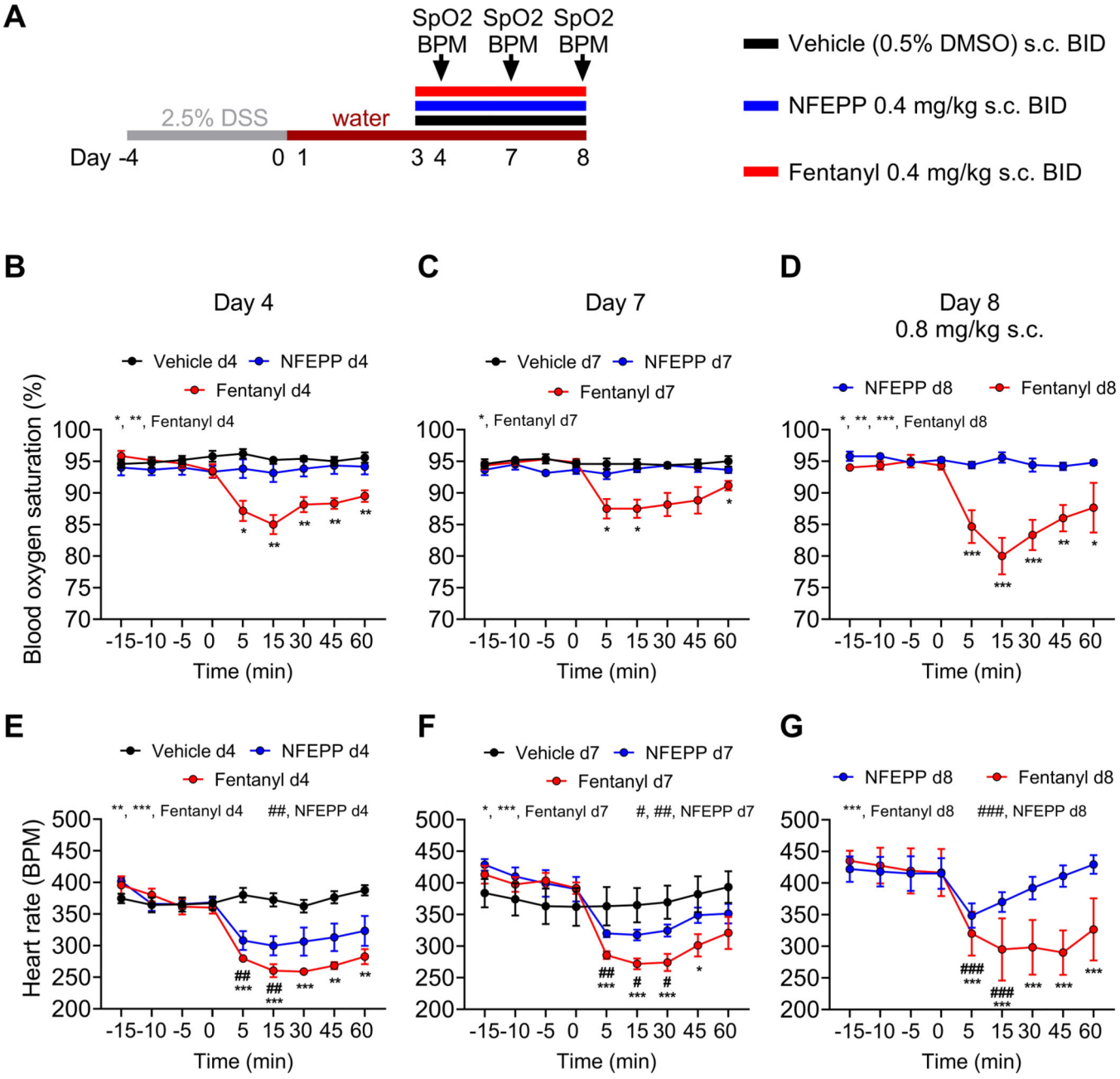

Fig. 5: On-target side effects of repeated NFEPP and fentanyl application during acute DSS colitis at different time points.

A. Study design with injection regimen (*color coded*). Pulse oximeter measurements were performed at day 4, day 7 and day 8 in vehicle (0.5% DMSO s.c. BID, N=5), NFEPP (0.4 mg/kg s.c. BID, N=6) and fentanyl (0.4 mg/kg s.c. BID, N=6) treated DSS colitis mice.

B-G. Effects of NFEPP and fentanyl on blood oxygen saturation (**B-D**) and heart rate (**E-G**) at different time points and concentrations. *Abbreviations: BID, bis in die (twice daily). BPM, beats per minute. DMSO, dimethyl sulfoxide. DSS, dextran sulphate sodium. SpO2, blood oxygen saturation. *, # p<0.05. **, ## p<0.01. ***, ### p<0.001. Two-way ANOVA, Bonferroni test. D, G: fentanyl: N=3; NFEPP: N=5.*

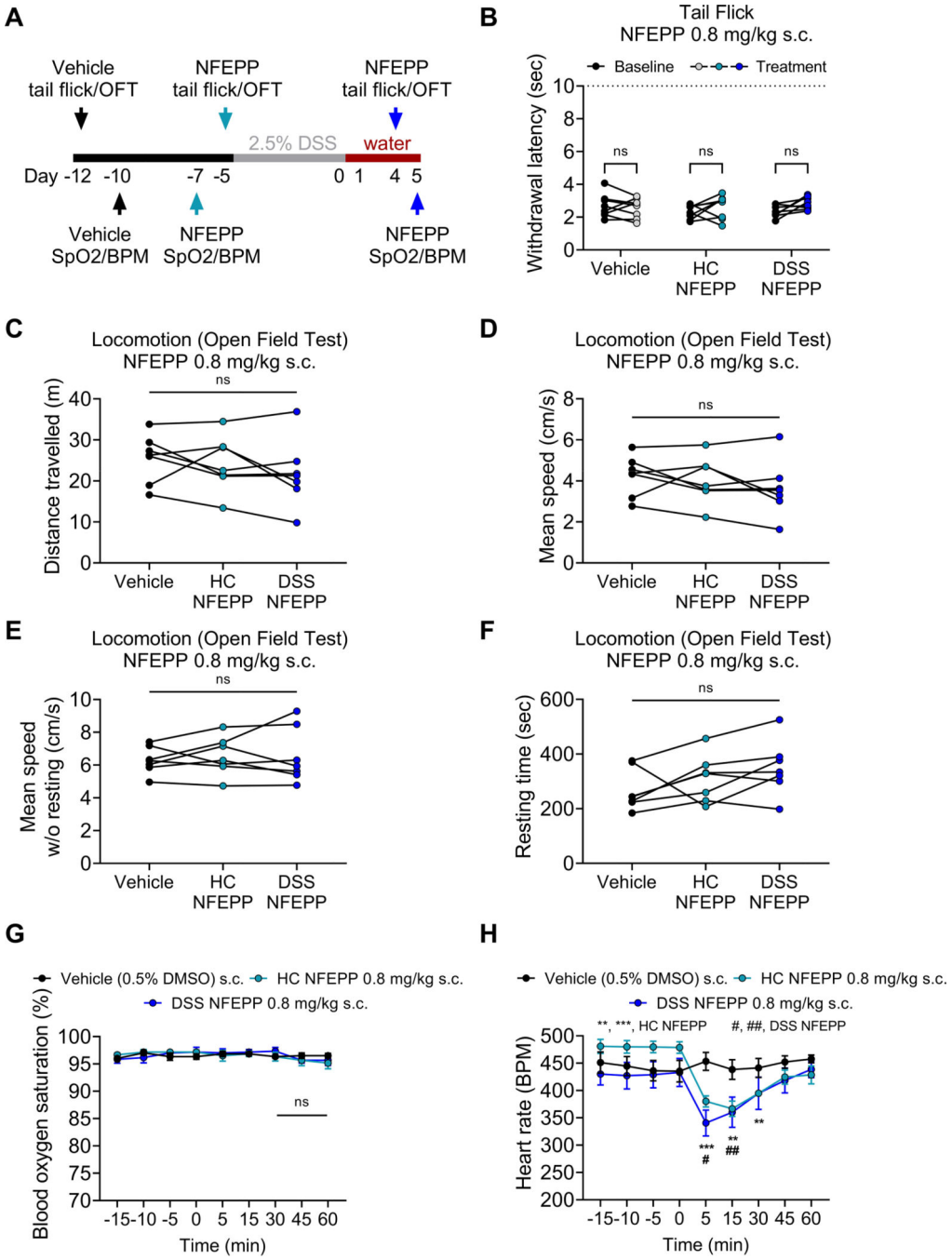

Fig. 6: On-target side effects of increased NFEPP doses in healthy control and acute DSS colitis mice.

A. Study design. Tail immersion assay (N=8), locomotor activity (N=7) and pulse oximeter measurements (N=6) were performed in the same mice at different time points. **B-H.** Effects of increased doses of NFEPP (0.8 mg/kg s.c.) on withdrawal responses to noxious heat in a tail immersion assay (**B**), locomotor activity (**C-F**), blood oxygen saturation (**G**) and heart rate (**H**) in healthy control (HC) and DSS colitis mice. *Abbreviations: BPM, beats per minute. DMSO, dimethyl sulfoxide. DSS, dextran sulphate sodium. OFT, open field test.*

*SpO2, blood oxygen saturation. # p<0.05. **, ## p<0.01. *** p<0.001. B, G-H: Two-way ANOVA, Bonferroni test. C-F: One-way ANOVA*

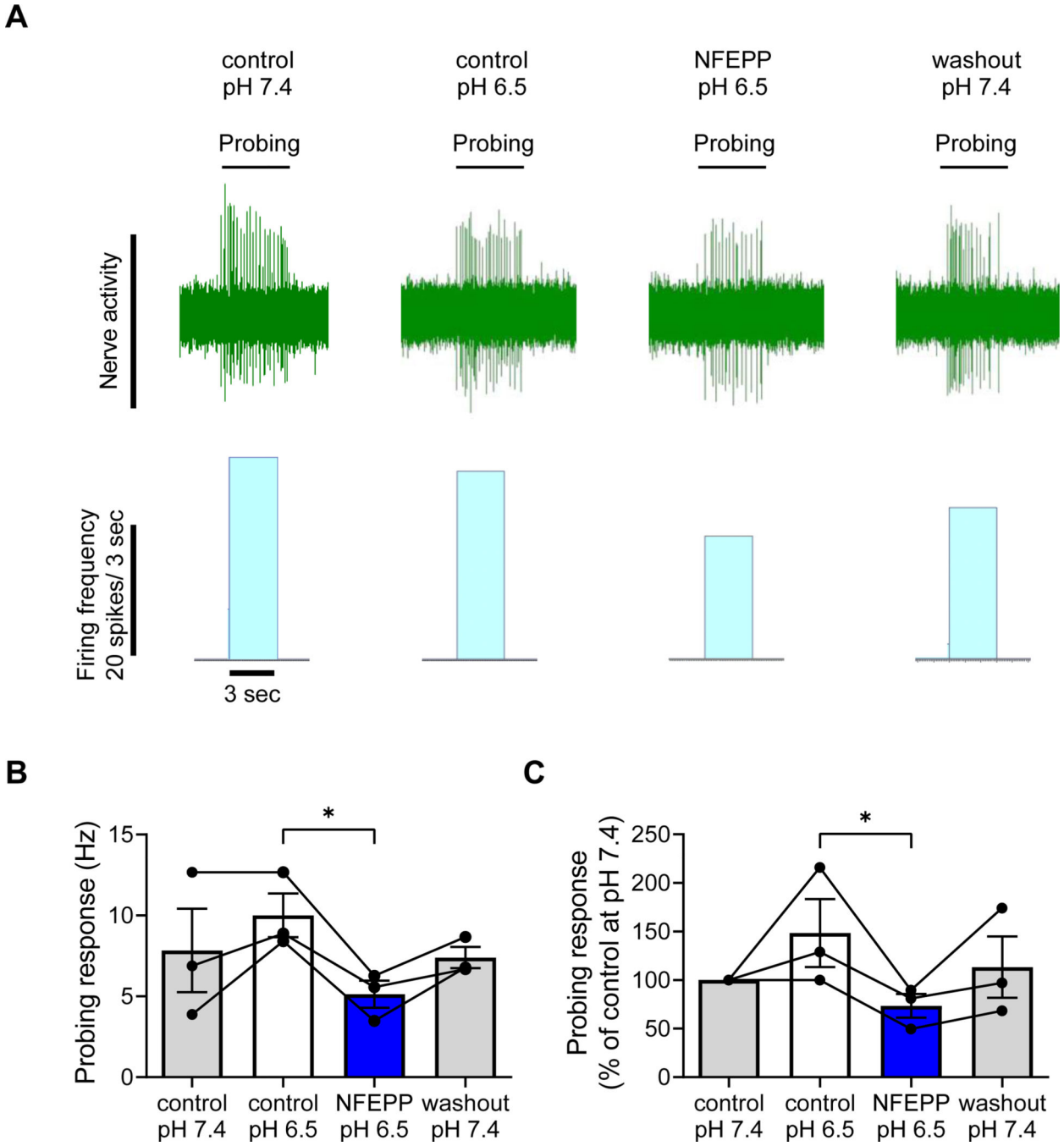

Fig. 7: Effects of NFEPP on human colonic nociceptors.

A. Representative traces and histograms of colonic afferent nerve firing in response to von Frey filament probing (10 g) at pH 7.4 (control), pH 6.5 (control), in presence of NFEPP (300 nM) at pH 6.5 and after washout at pH 7.4. **B-C.** Summary bar charts of afferent nerve probing responses (N=3) presented as Hz (**B**) and as % of control at pH 7.4 (**C**). *Abbreviations: Hz, Hertz. * p<0.05. Friedman test, Dunńs test.*